



HAL
open science

Sorption of Eu(III) on quartz at high salt concentrations

David Garcia, Johannes Lützenkirchen, Vladimir Petrov, Matthieu Siebentritt, Dieter Schild, Grégory Lefèvre, Thomas Rabung, Marcus Altmaier, Stepan Kalmykov, Lara Duro, et al.

► To cite this version:

David Garcia, Johannes Lützenkirchen, Vladimir Petrov, Matthieu Siebentritt, Dieter Schild, et al.. Sorption of Eu(III) on quartz at high salt concentrations. *Colloids and Surfaces A: Physicochemical and Engineering Aspects*, 2019, 578, pp.123610. 10.1016/j.colsurfa.2019.123610 . hal-02380916

HAL Id: hal-02380916

<https://hal.science/hal-02380916>

Submitted on 26 Nov 2019

HAL is a multi-disciplinary open access archive for the deposit and dissemination of scientific research documents, whether they are published or not. The documents may come from teaching and research institutions in France or abroad, or from public or private research centers.

L'archive ouverte pluridisciplinaire **HAL**, est destinée au dépôt et à la diffusion de documents scientifiques de niveau recherche, publiés ou non, émanant des établissements d'enseignement et de recherche français ou étrangers, des laboratoires publics ou privés.

1 **SORPTION OF Eu(III) ON QUARTZ AT HIGH SALT CONCENTRATIONS**

2 David García^{a,*}, Johannes Lützenkirchen^{b,*}, Vladimir Petrov^{c,*}, Matthieu Siebentritt^d, Dieter
3 Schild^b, Grégory Lefèvre^d, Thomas Rabung^b, Marcus Altmaier^b, Stepan Kalmykov^c, Lara Duro^b,
4 Horst Geckeis^b

5 a. Amphos 21, Carrer Veneçuela 103, 08019, Barcelona (ES)

6 b. Karlsruhe Institute of Technology (KIT) Institut für Nukleare Entsorgung (INE) ,Hermann-von-
7 Helmholtz-Platz 1, 76344 Eggenstein-Leopoldshafen (GER)

8 c. Lomonosov Moscow State University, Department of Chemistry, Leninskie gory, 1/3, 119991,
9 Moscow (RU)

10 d. PSL Research University, Chimie ParisTech — CNRS, Institut de Recherche de Chimie
11 Paris, 75005, Paris, France (FR)

12 13 **Abstract**

14 Sorption of Eu(III) onto quartz from highly saline solutions (up to 5M NaCl) has been studied by
15 sorption edges. The acid-base titrations of the solid surface suggest the rather unusual
16 presence of two different sites that has been the object of recent discussions in the literature.
17 Europium uptake results show the usual behaviour with a steep pH-edge and nearly complete
18 removal at sufficiently high pH. Previous spectroscopic data on this system suggest the
19 presence of two bidentate surface complexes with different proton stoichiometry. Based on this,
20 a self-consistent Surface Complexation Model (SCM) was fitted to the full set of experimental
21 data, from 0.1 to 5 M NaCl, using a coupled Pitzer/surface complexation approach. The Pitzer
22 model was applied to aqueous species. A Basic Stern Model was used for interfacial
23 electrostatics of the system, which includes ion-specific effects via ion-pair formation. Parameter
24 fitting was done using the general parameter estimation software UCODE coupled to a modified
25 version of FITEQL2 involving separate calculations of the respective ionic strength corrections.
26 At high ionic strength (>1 M), the surface potential is strongly screened by ion-pair formation
27 and the diffuse layer potential is negligibly low, which justifies the extension of the standard
28 electrostatic model to these harsh conditions. Overall, our model is able to describe the full set
29 of analysed data. It is expected that these first systematic data acquisition along with the
30 detailed modelling can serve as a benchmark for the modelling of future studies on sorption in
31 highly saline systems.

32 33 **Keywords**

34 Sorption, radionuclides, silica, high ionic strength, modelling, europium

* Corresponding author: Dr. David García. E-mail: david.garcia@amphos21.com. +34 935 830 500

* Corresponding author: Dr. Johannes Lützenkirchen. E-mail: johannes.luetzenkirchen@kit.edu. +49 721 608-2402

* Corresponding author: Dr. Vladimir Petrov. E-mail: vladimir.g.petrov@gmail.com

35 1. Introduction

36

37 Adsorption processes are important in retarding the potential migration of radionuclides from a
38 nuclear waste repository to the biosphere^{1,2}. Many studies have been carried out to
39 characterize the interactions of key radionuclides on many surfaces for a wide range of solution
40 compositions. The major body of the studies was performed with salt concentrations of 0.1M
41 and below³ and references therein). Surface complexation modelling approaches⁴⁻⁶ have
42 rationalized the adsorption of dissolved ions (such as heavy metal ions or radionuclides) in a
43 fashion similar to the treatment of aqueous complexation equilibria. In particular, on oxides,
44 surface ligands (surface hydroxyl groups) undergo protonation and/or deprotonation which
45 allow, along with an electrostatic model for the interface, the description of the charging curves
46 of the surfaces under study. The fundamental charging of oxide surfaces occurs via proton
47 uptake or release from the surface functional groups. The surface charge is pH dependent and
48 influenced by the electrolyte ions and increases with ionic strength. Adsorption of other solutes
49 like radionuclides is also pH dependent and affected by the variable charge of the surface. For
50 salt concentrations significantly higher than 0.1M there is no systematic data set to allow an
51 extension of the present modelling approaches to higher salt contents within a variable charge
52 model. In one case, data for sorption on montmorillonite were modelled using a combined Pitzer
53 and triple layer approach by Mahoney and Langmuir⁷. In Mahoney and Langmuir study's, the
54 data were more adequately modelled up to 4.0 M NaCl (encompassing data at 1.0 and 2.0 M
55 NaCl for the high concentration range) using activity coefficients calculated by the Davies
56 equation than by using Pitzer based activity coefficient models. It is unclear how the pH
57 measurements were actually done at the high salt level⁸ and if the charges were accurately
58 determined in the high salt level range, a Basic Stern model coupled to the Davies equation was
59 successful in describing the reported data also in 4.0 M NaCl⁹. The situation is different for
60 aqueous solubility and speciation of radionuclides where a large body of systematic
61 experimental data exists. In these cases, SIT and Pitzer modelling approaches set
62 thermodynamic frameworks that can be applied to performance assessment for repositories in
63 salt formations¹⁰ to include solubility limits and concomitant effects of aqueous solution
64 complexation effects. The importance of obtaining accurate data and using consistent
65 thermodynamic data to model them is obvious. For the aqueous solution this concerns the
66 measurement of the proton activity, which is a master variable, and which is not trivial at high
67 salt levels, and the calculation of correct activity coefficients¹¹.

68 Radionuclide retention due to surface reactions is typically represented in Performance
69 Assessment calculations by the equilibrium distribution coefficient (K_d), which is a quotient
70 between the adsorbed concentration of radionuclide (mass of radionuclide per unit mass of
71 solid) and the aqueous concentration of radionuclide (mass of radionuclide per unit volume of
72 solution)¹². Overall, K_d values lump together various processes (e.g. surface complexation, ion-
73 exchange, precipitation, co-precipitation, etc.) and do not provide appreciable insight into the
74 retention mechanism. Alternatively, radionuclide retention processes can be assessed through

75 the use of surface complexation models. Such approach, based on the definition on a
76 mechanistic reaction model, can represent a variety of retention reactions (equilibrium and
77 kinetic). It has become highly desirable to approach adsorption in more concentrated solutions,
78 covering intermediate (0.1-1 M) and high ionic strength (>1 M), by similar procedures. This
79 involves collection of experimental data in a systematic way on a model system in a first step
80 and a subsequent attempt to rationalize the data in terms of a surface complexation model.
81 As a model surface, quartz is studied in this work. Quartz presents well-known surface
82 properties, with surface functional groups also present on the surface of clays and clay
83 minerals. On the other hand, trivalent lanthanides, and more precisely, Eu has been selected as
84 adsorbing solute of interest for the adsorption studies. This trivalent lanthanide cation is often
85 used as a proxy for the radionuclides Am and Cm, which constitute an important fraction of the
86 minor lanthanides/actinides present in the high-level liquid waste generated during the
87 reprocessing of spent nuclear fuel¹³. In the scenario of a repository failure, these radionuclides
88 could migrate away from the waste disposal site, finally entering the geosphere. During this
89 migration process they will be interacting with the surrounding host-rock minerals.
90 Consequently, a reliable understanding of their behaviour in contact with surfaces is crucial
91 whenever retention processes are to be taken advantage of in the Safety Case for a given
92 repository. Extensive studies have been carried out on the uptake of trivalent actinides onto
93 mineral surfaces under different conditions¹³⁻¹⁸, but a study for high salt content on silica
94 minerals is missing. In Germany and some other countries (Canada, USA, etc.) some options
95 for repositories in areas that would involve highly saline aqueous solutions have been discussed
96 and experimental data and models for treating such systems are required.

97

98 It is expected that such a model can be applied in Performance Assessment for a nuclear waste
99 repository in highly saline environment in a similar way as is nowadays envisaged or applied for
100 sorption from low ionic strength solutions in the licensing process for nuclear waste repositories
101 or practised in general environmental contexts with respect to contaminant transport. Data on
102 Eu adsorption on clay surfaces have been recently published up to high ionic strength and were
103 modelled by a non-electrostatic surface complexation model coupled to the Pitzer approach¹⁶.
104 While the coupling itself is rather a technical problem, the more interesting scientific issue is
105 how traditional electrostatic models perform at high salt concentrations. One issue is whether
106 coupled models yield a good fit to experimental data over the full range of background
107 electrolyte content. Another arises from the fact that the application of the Gouy-Chapman-type
108 treatment that is part of many of those models is beyond the limits of the underlying theory. For
109 this reason, the constant capacitance model has been traditionally used as the equivalent of the
110 constant ion medium approach in solution studies to treat the interfacial electrostatics at high -
111 medium concentrations¹⁹. Although the constant capacitance model allows for variable ionic
112 strength in a semi-predictive way²⁰, it is preferable to have a fully consistent set of surface
113 complexation parameters to describe a given system. We therefore test a Basic Stern model to
114 describe electrostatics at the mineral water interface up to high salt concentrations. Hiemstra

115 and co-workers⁹ modelled data on silica from Bolt²¹ up to 4M NaCl applying conventional
116 activity corrections involving the Davies-equation. At the highest salt level, such approaches fail
117 to correctly describe the activity corrections of the dissolved species. Except for the works of
118 Schnurr et al.¹⁶ and Zoll and Schifj²², on clay minerals and algae respectively, we have no
119 knowledge of a consistent treatment of the activity corrections up to salt brines in an adsorption
120 study. This work therefore is the first attempt to couple Pitzer equations with an electrostatic
121 model for the interface. The use of Pitzer equations to calculate activity coefficients at high ionic
122 strength conditions is preferred because this model allows a robust description of the complex
123 ion-interaction processes in saline media. As will be seen later, the model performs very well for
124 our system. Furthermore, due to the high salt content, the impact of the Gouy-Chapman part
125 (i.e. the diffuse part of the double layer) is of minor importance, since the fundamental charge
126 caused by proton ad- and desorption from surface functional groups is sufficiently screened by
127 counter-ion adsorption.

128

129 **2. Materials and Methods**

130

131 **2.1 Materials**

132

133 Commercially available MINUSIL 5 particles (pure quartz particles of nominal 5 μm size) were
134 obtained from U.S. silica company. The solids were washed several times with dilute HNO_3
135 solutions, dried and checked for the absence of impurities by XPS. The XPS spectra (not
136 shown) did not reveal any significant impurities on the pre-treated particles. The specific surface
137 area (measured by BET using Nitrogen gas) of the pre-treated particles was $6.5 \text{ m}^2/\text{g}$.

138

139 **2.2 Surface titrations and zeta potentials measurements**

140

141 The MINUSIL solids were titrated at different NaCl concentrations (0.1, 1, 3 and 5M). Titrations
142 were carried out in fast mode with small additions of titrant and short waiting times between
143 additions. Calibration of the measurement set-up was done with standard procedure but
144 considering the "A"-factor which allows to correct operational, measured pH values at high ionic
145 strength to pH_c ($-\log[\text{H}^+]$)²⁰. The set-up was purged by purified and humidified Argon to avoid
146 intrusion of carbon dioxide and limit evaporation. The data treatment followed standard
147 procedures. The values for $\text{p}K_w$ at the different ionic strengths were calculated using the Pitzer
148 formalisms. The Pitzer parameters were those used by Schnurr et al.¹⁶ (for the Am-Na-Cl-
149 system). They are self-consistent, and consistent between the treatment of the titration data and
150 the modelling of our experimental titration and adsorption data. The raw data yielded the relative
151 surface charge as a function of pH_c . For the modelling it is necessary to determine the absolute
152 charge. It is not straightforward to decide how to treat the data at these high salt contents, as
153 several pH-scales would be possible besides the pH_c scale. Plotting the relative data on any of
154 these scales could yield a common intersection point. In the case of standard quartz no

155 common intersection point is expected, but the observed plateau down to low pH is usually set
156 to absolute zero surface charge. Our data do not show classical quartz behaviour, therefore no
157 clear acidity scale to define common intersection points can be defined. A consistent way to fix
158 the absolute charge is to use the Pitzer pH scale within a model and involve zeta-potential
159 measurements, which give an absolute value of the surface charge within the shear-plane.
160 The DT-300 system from Quantachrome/Dispersion Technology was used for the
161 electroacoustic experiments. Before each new measurement, a calibration of the probe is done
162 in a particle-free solution, and the background current is automatically subtracted from the
163 suspension measurements. Moreover, ultrasounds are applied for 3 min in the suspensions
164 before any experiment using a sonotrode (UP100H model from Hielscher). To calculate zeta
165 potential from electroacoustic measurements, a bimodal size distribution has been used,
166 resulting from laser diffraction granulometry. The pH was measured in the usual way, i.e. by
167 calibrating against three commercial buffers. With the lower ionic strength, no extra corrections
168 were required.

169

170 **2.3 Batch Sorption studies**

171

172 Eu sorption onto MINUSIL particles was studied in NaCl solutions of different ionic strengths:
173 0.1, 1, 3 and 5M. The total concentration of Eu in all cases was $1 \cdot 10^{-7}$ M, the solid to liquid ratio
174 was 10g/L, and pH_c values were varied in the range from 2.5 to 8.0 by HCl and NaOH solutions.
175 The pH_c values were determined using the known "A"-factors as described in the previous
176 section.

177

178

179 **2.4 Speciation calculations and surface complexation modelling**

180

181 Thermodynamic data ($\log \beta^0$ values) used in this work are identical to those used by Schnurr et
182 al.¹⁶. We summarize the $\log \beta^0$ values for the aqueous Eu-species, which have been taken from
183 the NEA compilation for Americium²³ (see Table 1). The Pitzer activity coefficients were used
184 as indicated above. Europium and Americium, generally featuring analogous aqueous species
185 with comparable structures, are usually treated within a common scheme to describe ion-
186 interaction processes. The potential dissolution of quartz may result in the formation of silicic
187 acid that may act as inorganic ligand for cations. However, in a related study it was found that
188 addition of dissolved silica is required to affect the speciation in this system¹⁷. Moreover,
189 increasing the system ionic strength largely decrease the stability of ternary aqueous species
190 Eu-H₂O-Si. Thus, no attempt was made to include Si aqueous speciation in the model, i.e.
191 ternary aqueous or surface species were not considered.

192 **Table 1.** $\log \beta^0$ used for calculating the aqueous speciation of Eu(III).

Reaction	$\log \beta^0$
$\text{Eu}^{3+} + \text{H}_2\text{O} \leftrightarrow \text{Eu}(\text{OH})^{2+} + \text{H}^+$	-7.20
$\text{Eu}^{3+} + 2\text{H}_2\text{O} \leftrightarrow \text{Eu}(\text{OH})_2^+ + 2\text{H}^+$	-15.1
$\text{Eu}^{3+} + 3\text{H}_2\text{O} \leftrightarrow \text{Eu}(\text{OH})_3(\text{aq}) + 3\text{H}^+$	-26.2
$\text{Eu}^{3+} + 4\text{H}_2\text{O} \leftrightarrow \text{Eu}(\text{OH})_4^- + 4\text{H}^+$	-40.6
$\text{Eu}^{3+} + \text{Cl}^- \leftrightarrow \text{EuCl}^{2+}$	0.24
$\text{Eu}^{3+} + 2\text{Cl}^- \leftrightarrow \text{EuCl}_2^+$	-0.74

193

194 Quartz surface protonation is modelled with a 2-site protolysis model²⁴. The MINUSIL sample
 195 used in this study presents two distinct types of functional groups that govern the reactions
 196 taking place at the quartz surface. A basic Stern model is used for interfacial electrostatics of
 197 the system, which includes ion-specific effects via the formation of ion-pairs between ionized
 198 surface functional groups and ions of the background electrolyte²⁵. For the fundamental
 199 charging the titration and zeta-potential results were fitted simultaneously. As previously
 200 explained, a major problem in the treatment of the titration data is that the absolute charge
 201 cannot be determined. Zeta-potentials are an absolute measure of the net-charge within the
 202 shear-plane and are affected by the proton ad- and desorption reactions. The coupling of the
 203 various data sets via UCODE is possible and allows the relative charging data obtained in the
 204 titrations²⁶ to be transformed to absolute values, while simultaneously fitting capacitance and
 205 stability constants. Site densities were constrained as described below.

206 Metal ion adsorption is modelled by applying those parameters derived from titration results, i.e.
 207 capacitance and surface hydrolysis constants, and fitting a hypothetical surface complex
 208 stoichiometry with a charge distribution to the experimental Eu uptake data. Parameter fitting is
 209 done using the general parameter estimation software UCODE²⁷ coupled to a modified version
 210 of FITEQL2²⁸.

211 No separate activity corrections apart from electrostatic factors are applied to the surface
 212 species, i.e. in the mass law equations for adsorption reactions only activity coefficients for
 213 dissolved species and activities of water are considered in the calculation of the ionic strength
 214 dependence of stability constants for surface species. The activity coefficients were separately
 215 calculated using the Pitzer formalism and available self-consistent databases, as described in
 216 detail elsewhere¹⁶. The resulting activity coefficients were then used to calculate conditional
 217 stability constants at infinite dilution, or corrections factors to stability constants that were to be
 218 fitted. Fitting thus yields the stability constants at infinite dilution.

219

220 **3. Results**

221

222 **3.1 Surface titrations and zeta potentials**

223

224 Surface titration results are presented as symbols in Figure 1 in terms of surface charge (in
225 $\text{mC}\cdot\text{m}^{-2}$) vs pH_c . The charging curves agree with some previously published studies²⁹, but only
226 differ from the bulk of the literature data for quartz and silica, which show the deprotonation step
227 at high pH. Our data are surprising in the sense that a distinct two step behaviour is observed.
228 Usually such stepwise deprotonation is overshadowed by electrostatics and/or site distributions
229³⁰. Ong et al.²⁹ used second harmonic generation to study the interface between fused silica
230 and sodium chloride solutions as a function of pH. They found a two step-behaviour and
231 reported $\log \beta$ values of -4.5 and -8.5 in 0.5 M NaCl and a ratio of 1:4 between the two types of
232 sites. There are various independent studies that report the existence of two distinct sites on
233 various silica samples^{24,31-35}. Our proposed model involves two sites, as does the Ong et al.
234 model, and Figure 1 and Figure 3 show the fits to the surface titrations and the zeta-potentials.
235 Solid lines in Figure 1 represent the best fit results. The SCM parameters used in the fitting are
236 detailed in Table 2. The site densities were constrained according to Ong et al. assuming a total
237 site density of $4.6 \text{ sites}/\text{nm}^2$ ¹⁸.

238 In the acidic pH range ($\text{pH}_c < 6$), for the same pH_c value the negative surface charge increases
239 when increasing the ionic strength of the system. A further decrease in the negative charge was
240 observed in the basic pH range ($\text{pH}_c > 7$). This behaviour can be described by the speciation
241 scheme presented in Figure 4. Deprotonated species are predominant in both, acidic and basic,
242 pH_c conditions. We will refer to the more acidic site as the hydrophobic site x. Counter-ions (Na^+
243 and Cl^-) adsorption has also been considered (Table 2).

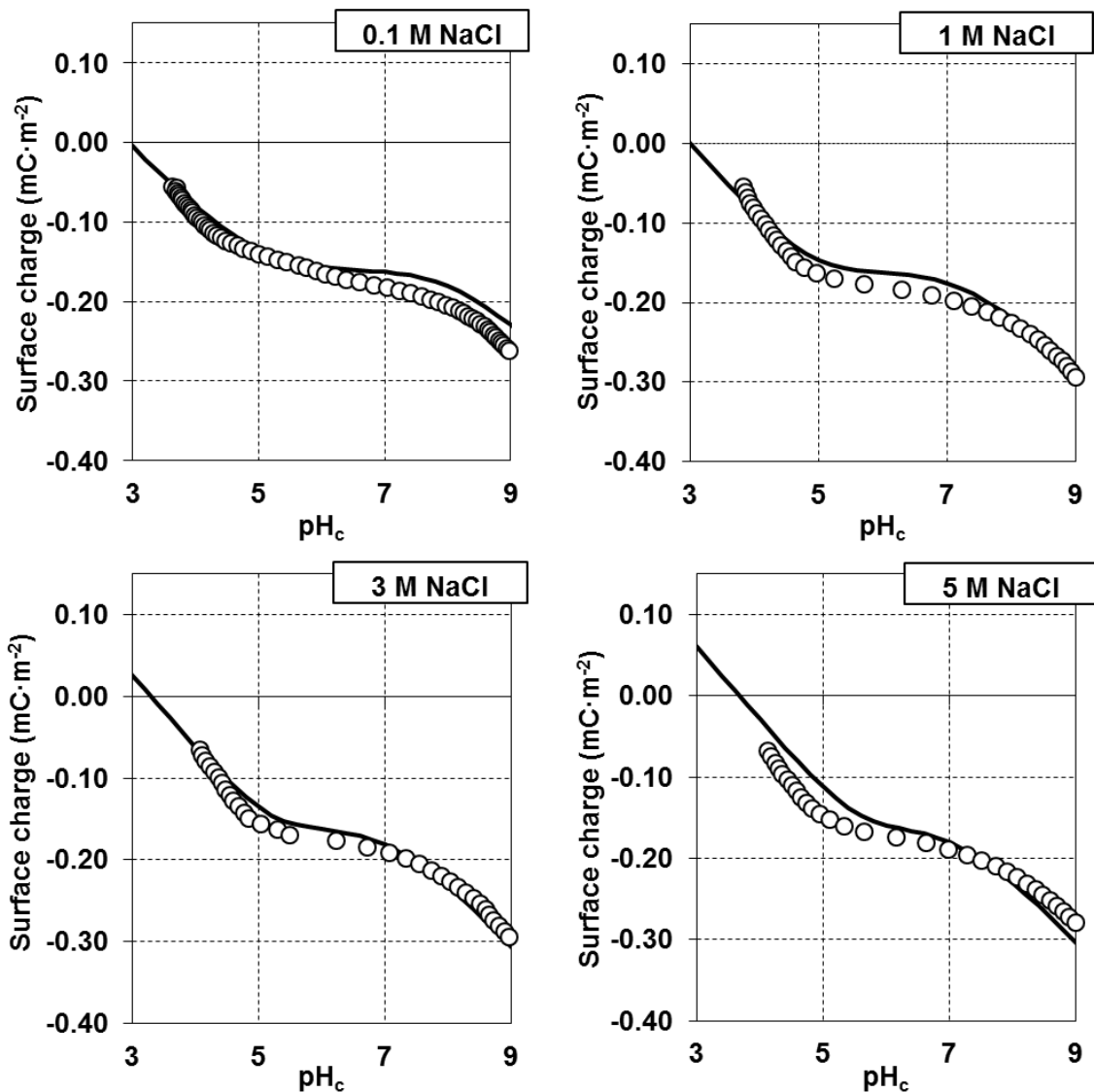
244 The pK_a values in our modelling have been placed close to those obtained by Ong et al. within a
245 Diffuse Layer model for data at 0.5M NaCl²⁹. The site labelled y is the "usual" silanol site with
246 an assigned pK value of about 8.5 and sodium association is also in the range typically reported
247^{13,17,29}. The "hydrophobic" site involves a pK value fixed at about 4.0. Overall, the two pK values
248 for deprotonation extracted from our experimental data (i.e. 4.0 and 8.5) agree with independent
249 data reported in the literature, i.e. 2-3 and 9-10 from³⁵, 4.5 and 8.5 from²⁹, 5.5 and 9.0 from³¹.

250 To be able to model the data we had to involve rather strong counter-ion association with the
251 hydrophobic site. There have been recent reports on ion-specific effects on fused silica in the
252 acidic range³⁶, which may be taken as support for our findings. A more direct indication from
253 AFM measurements where the two sites were also identified on one sample shows that cation-
254 specificity is inversed³⁷ and that the more acidic site is indeed showing the sequence expected
255 for a hydrophobic surface³⁸.

256 **Table 2.** Parameters and reactions used to model the amphoteric behaviour of quartz surface
 257 with an electrostatic SCM model at infinite dilution. In italics fitted parameters.

Reaction	log K^0
$\equiv\text{Si}_x\text{OH} + \text{H}^+ \leftrightarrow \equiv\text{Si}_x\text{OH}_2^+$	-1.3 ^a
$\equiv\text{Si}_x\text{OH} \leftrightarrow \equiv\text{Si}_x\text{O}^- + \text{H}^+$	-4.0 ^b
$\equiv\text{Si}_y\text{OH} \leftrightarrow \equiv\text{Si}_y\text{O}^- + \text{H}^+$	-8.5 ^c
Parameter	
Site x (sites·nm ⁻²)	1.0
Site y (sites·nm ⁻²)	3.7
Capacitance (F·m ⁻²)	2.0
Specific surface area (m ² ·g ⁻¹)	6.5
Shear plane distance parameter ^d	0.03

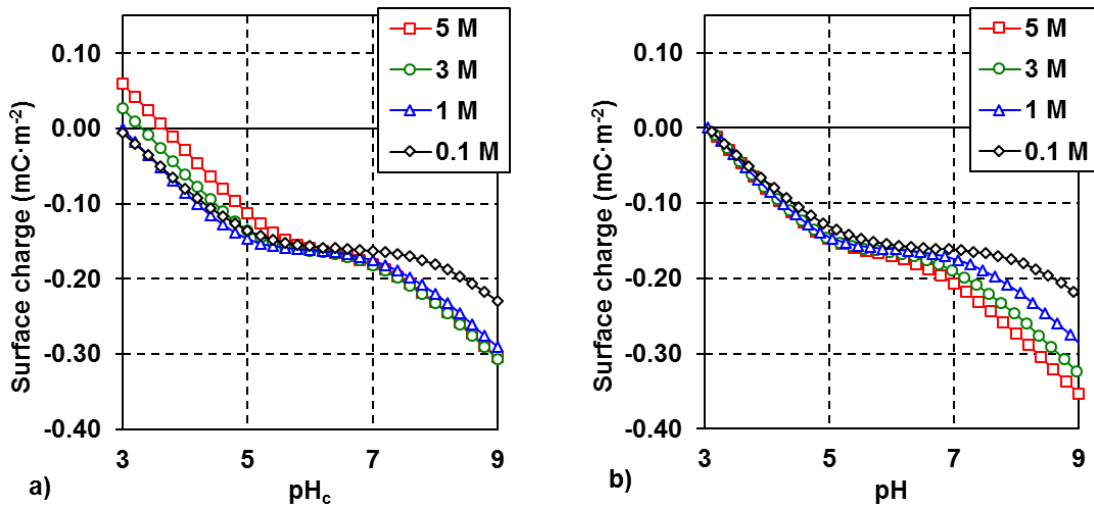
258 a. Counter ion (Cl⁻) constant (log K) for $\equiv\text{Si}_x\text{OH}$ is 1.9; b. Counter ion (Na⁺) constant (log K) for
 259 $\equiv\text{Si}_x\text{OH}$ was 5.4; c. Counter ion (Na⁺) constant (log K) for $\equiv\text{Si}_y\text{OH}$ is 1.5. d. ratio between shear-
 260 plane distance and Debye-length; a value close to zero suggests that the model inherent shear-
 261 plane is close to the (theoretical) onset of the diffuse layer.
 262



263 **Figure 1.** Surface charge density as a function of pH_c for MINUSIL quartz particles at different
 264 ionic strengths (0.1-5M) in NaCl medium. Symbols stand for the experimental results, while lines
 265 are the best fit model using Table 2 parameters and Pitzer activity coefficients for aqueous
 266 solution speciation.

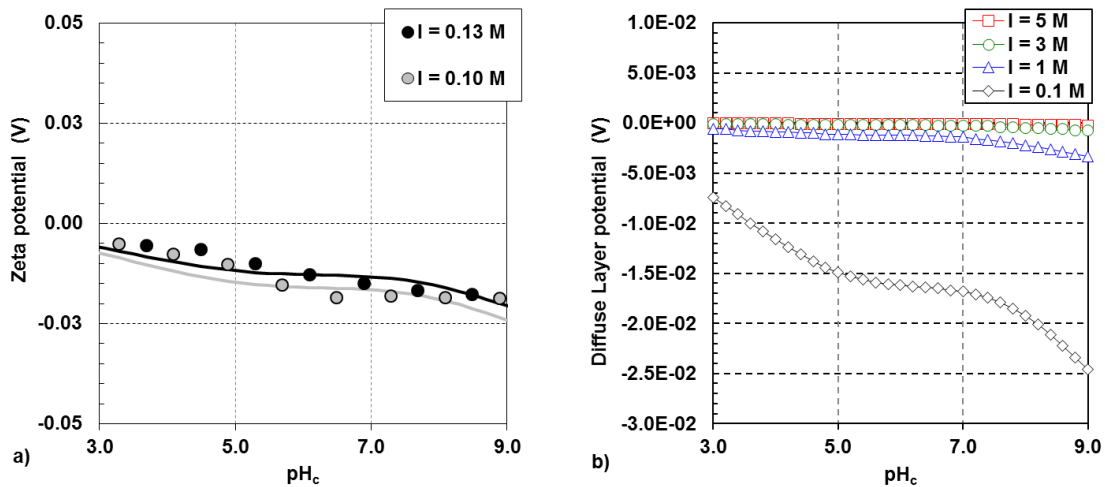
267

268 A comparison between surface charge as a function of pH_c (concentration scale) respectively
 269 pH (activity scale, here Pitzer pH scale) is presented in Figure 2a and Figure 2b respectively.
 270 Figure 2 highlights that the mode of presenting the data (either on the concentration or on the
 271 activity scale) has some repercussion on how to classify the observations. On the concentration
 272 scale, there is strong effect of salt on the hydrophobic site, while there is no effect for the
 273 hydrophilic site at salt contents of 1M and above (Figure 2a). On the Pitzer-activity scale, hardly
 274 any effect of salt is observed on the hydrophobic site, while the hydrophilic site clearly follows
 275 the trend found in comparable studies at salt contents below 1M. The choice of the scales also
 276 has repercussions on how to classify specific adsorption as will be discussed later.



278 **Figure 2.** Calculated surface charge density as a function of a) pH_c and b) pH (Pitzer pH scale)
 279 for MINUSIL quartz particles at different ionic strengths (0.1-5M) in NaCl medium. Table 2
 280 parameters and Pitzer activity coefficients for aqueous solution speciation have been used in
 281 these calculations.

282

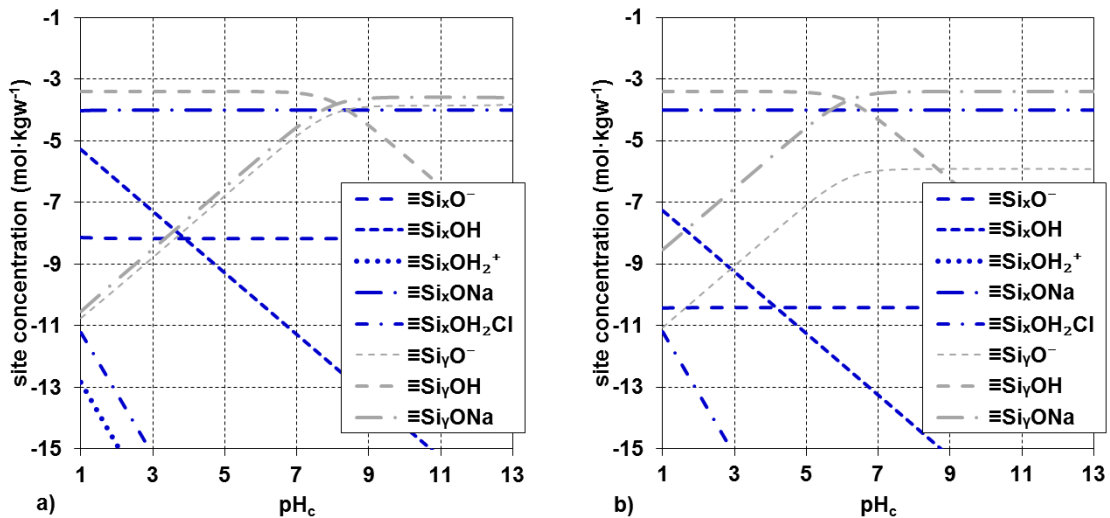


283 **Figure 3.** a) Zeta potentials as a function of pH_c for two different NaCl concentrations, 0.1 and
 284 0.13M. Symbols stand for experimental data while lines are the predictions by the SCM detailed
 285 in Table 2. b) Diffuse Layer potentials as a function of pH_c for the different NaCl concentrations,
 286 from 0.1 to 5M, studied in the present work.

287

288 Figure 3 shows calculated interfacial potentials based on the present model. Figure 3a presents
 289 the measured zeta-potentials for the sample at approximately 0.1M NaCl with the concomitant
 290 model calculations, showing a rather good fit. Figure 3b shows the model inherent diffuse layer
 291 potentials for the various NaCl concentrations used in the titrations. Due to the strong ion-

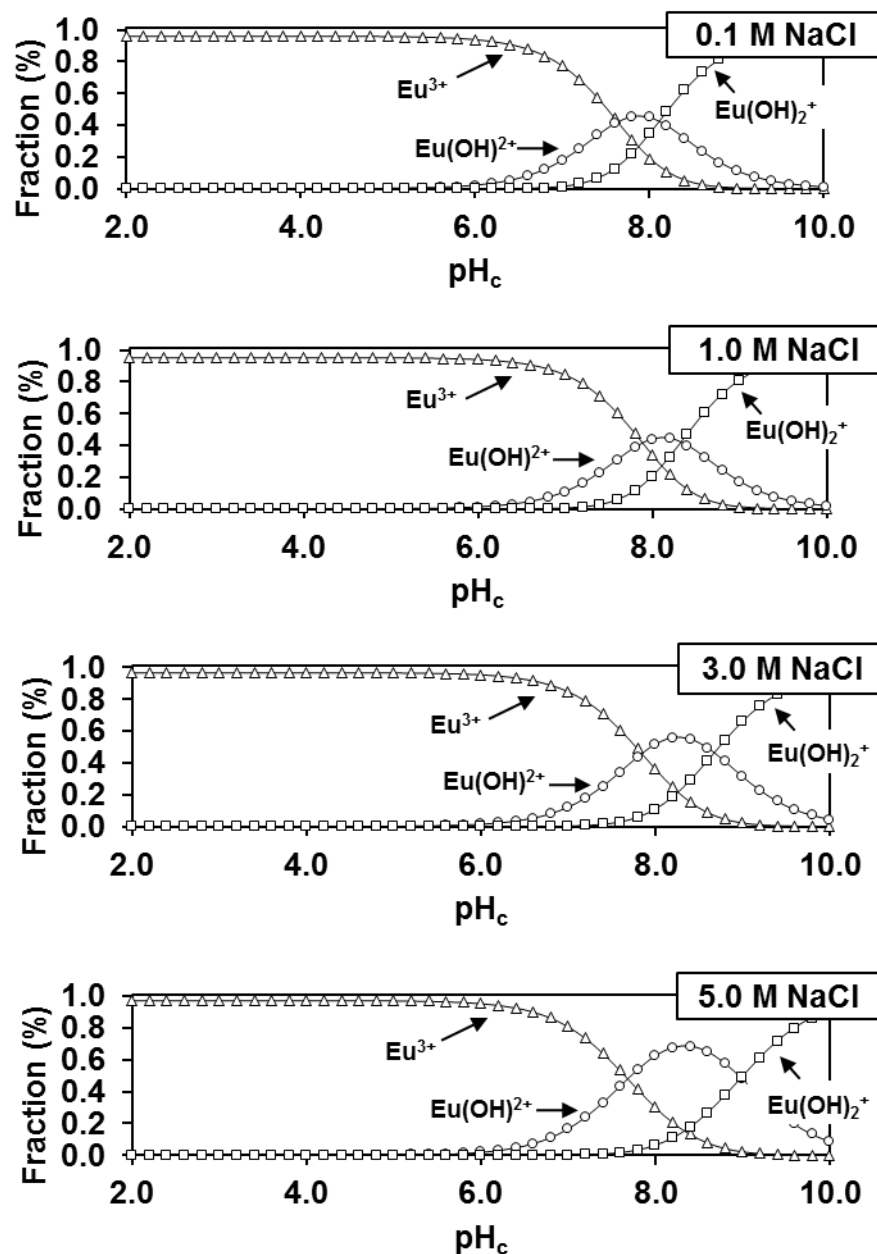
292 pairing there is a strong drop in the interfacial potential up to the head end of the diffuse layer.
 293 The diffuse layer potentials become very low for $I \geq 1\text{M NaCl}$. This justifies the application of the
 294 conventional diffuse layer, mainly because the diffuse layer potential becomes insignificant. The
 295 zeta-potentials can be described by a shear-plane distance parameter close to zero, which
 296 means the shear plane is nearly identical with the head end of the diffuse layer.
 297 Figure 4 shows the surface speciation according to the model for 0.1M (Figure 4 - a) and 5M
 298 (Figure 4 - b). The high salt content clearly drives the ion-pairs with sodium to control the
 299 speciation on the hydrophilic site.
 300



301 **Figure 4.** Silica surface speciation as a function of pH_c according with the model presented in
 302 Table 2, at a) 0.1M NaCl and b) 5.0M NaCl.

303
 304 **3.2 Aqueous speciation of Eu**

305
 306 Aqueous Eu speciation over a wide range of pH_c is shown in Figure 5 for the different NaCl
 307 concentrations. Increasing the ionic strength has not an important effect under acid conditions.
 308 The two aqueous species, EuCl₂⁺ and EuCl₂⁺, are negligible even at Cl concentrations as high
 309 as 5M (not shown in the Figure). In the basic pH range (pH_c>8), within our speciation scheme,
 310 minor differences can be observed with the increase of ionic strength. As pointed out by
 311 Schnurr et al.¹⁶, the Pitzer parameters for the chloride complexes in NaCl systems are not
 312 complete, but the resulting effects on europium speciation are minor.
 313



314

315 **Figure 5.** Aqueous speciation of Eu vs. pH_c based on the available thermodynamic parameters.

316 Fraction of Eu species at different NaCl concentrations for [Eu]_T=1·10⁻⁷M. Thermodynamic data

317 are reported in Table 1.

318 A more interesting feature in Figure 5 is that with increasing salt content, the model predicts a

319 consistent increase in the stability of the first hydrolysis species over the other species. Clearly

320 this species increases from below 50 % (at 0.1M) to almost 70 % (at 5M) of the total Eu in

321 solution at 5M NaCl. The first hydrolysis species has often been considered relevant for the

322 onset of adsorption³⁹, and linear free energy relationships are often used to relate surface

323 complexation constants with the first hydrolysis constant in the case of cations. This would

324 suggest stronger adsorption of Eu in the 0.1M NaCl system at a given pH_c compared to the

325 higher ionic strengths.

326

327 3.3 Adsorption of Eu onto MINUSIL particles

328

329 Experimentally obtained Eu sorption edges are presented in Figure 6 (symbols) as fractional
330 uptake vs pH_c in the various NaCl media (from 0.1 to 5 M). A shift in the sorption edges to
331 higher pH_c is found on the log proton concentration (pH_c) scale with increasing ionic strength. In
332 the four studied ionic strengths Eu adsorption onto quartz starts at $\text{pH}_c \sim 4$ and reaches almost
333 95% at $\text{pH}_c \sim 6$. At more basic conditions, nearly complete uptake is observed. As expected
334 based on the aqueous speciation, enhanced adsorption is observed at the low pH_c in 0.1M NaCl
335 compared to the higher ionic strengths.

336 The electrostatic SCM developed for simulating Eu uptake onto quartz by using the surface
337 protonation model and the Eu aqueous speciation described above includes two bidentate
338 surface complexes (Table 3). The stoichiometry was taken from Stumpf et al.¹⁷ and the stability
339 constants have been fitted to the basic (i.e. classical silanol) site. No adsorption on the
340 hydrophobic site was considered. This agrees with the recently reported cation adsorption
341 sequence³⁷. Charge Distribution (CD) is applied in the SCM and CD factors are optimized as
342 well. Model results are shown as solid lines in Figure 6, and show very good agreement with the
343 experimental results.

344 **Table 3.** Parameters and reactions used to model Eu sorption onto quartz surface with an
345 electrostatic SCM model at infinite dilution. The fitted parameters are given in italics. The charge
346 distribution is given in terms of the charge of the Europium charge that is allocated to the
347 surface plane.

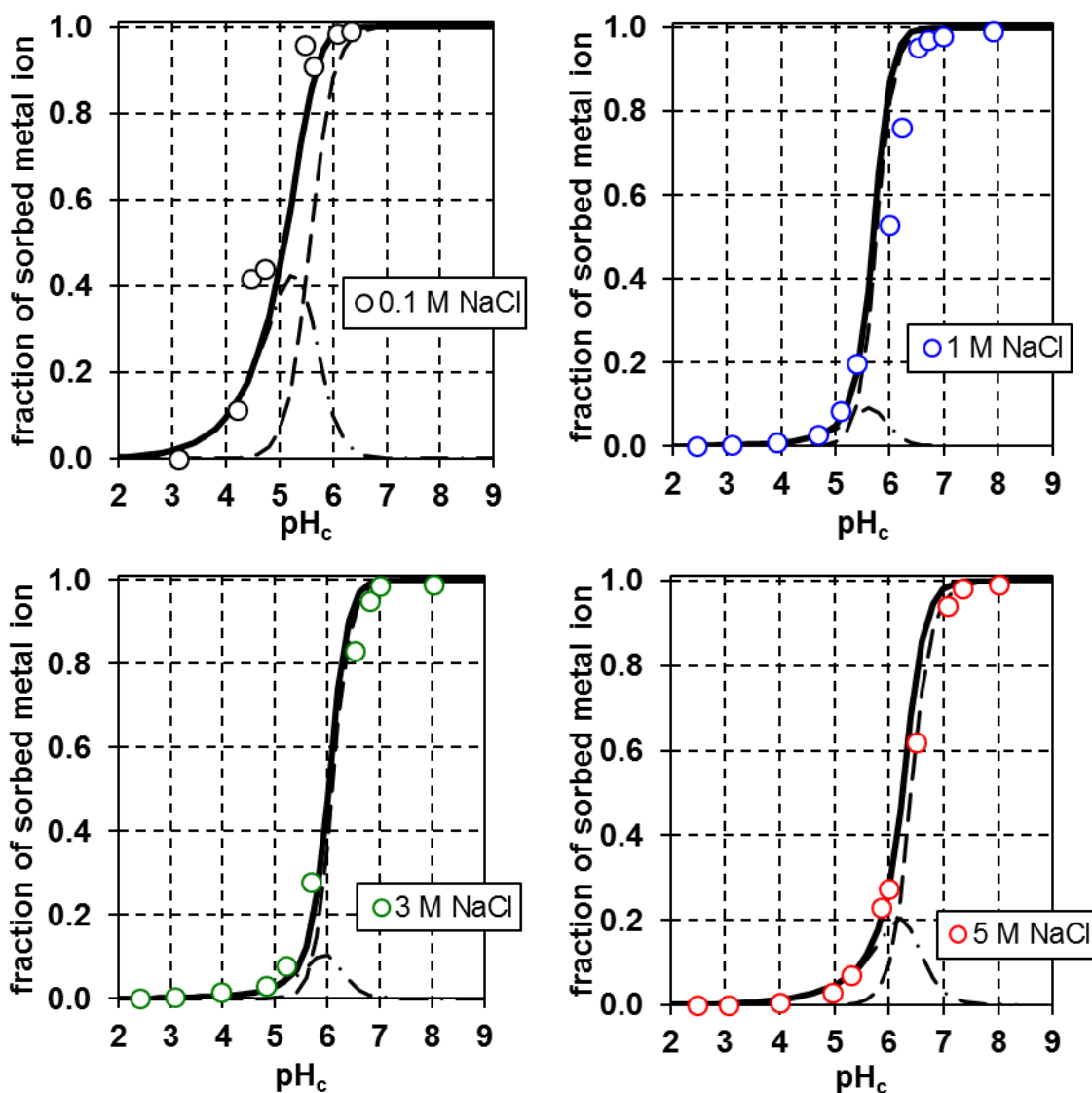
Reaction	$\log K^0$	$\Delta z_{0,\text{Eu}}$
$2(\equiv\text{Si}_y\text{OH}) + \text{Eu}^{3+} \leftrightarrow 2(\equiv\text{Si}_y\text{O})\text{HEu}^{2+} + \text{H}^+$	<i>-0.65</i>	<i>0.36</i>
$2(\equiv\text{Si}_y\text{OH}) + \text{Eu}^{3+} + \text{H}_2\text{O} \leftrightarrow 2(\equiv\text{Si}_y\text{O})\text{EuOH}^+ + 2\text{H}^+$	<i>-10.02</i>	<i>0.02</i>

348

349 As pointed out above, in previous work¹⁷ the same bidentate model in terms of stoichiometry
350 was already used to describe Am(III) and Cm(III) sorption onto another quartz sample. The
351 authors at the time confirmed the presence of at least two Eu surface complexes on the quartz
352 surface by means of TRLFS measurements and the TRLFS also suggested the applied proton
353 stoichiometry in going from the first to the second surface complex. Differences in the model
354 concepts and parameters, e.g. the use of Pitzer instead of Davies for activity corrections, or in
355 the model parameters, e.g. system capacitance, silica surface protonation, CD factors explain
356 the observed discrepancies in model parameters between the study of Stumpf et al. and ours.
357 Considering the CD-factors, the present results indicate a more outer-sphere-type surface
358 complex formation for the same overall stoichiometry compared to Stumpf et al.¹⁷.

359 In a more recent work, Kar and Tomar¹³ modelled Cm(III) sorption onto silica at 0.1M NaCl and
360 reported the formation of two distinct monodentate surface complexes, $\equiv\text{SiOCm}^{2+}$ and
361 $\equiv\text{SiOCm}(\text{OSi}(\text{OH})_3)_2$, with $\log K$ of -2.53 and -7.94 respectively. These authors applied a Diffuse

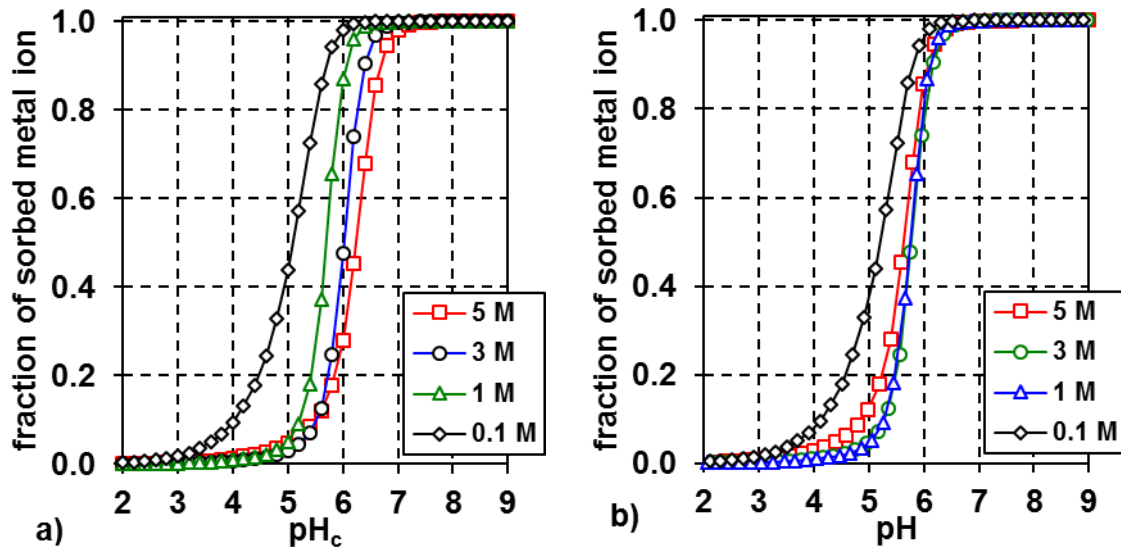
362 Layer Model (DLM) for describing the interfacial electrostatics of the system. The formation of
 363 the ternary aqueous species $\text{Cm-H}_2\text{O-Si, } \equiv\text{Si}_x\text{OCm(OSi(OH)}_3)_2$ as in the study Kar and Tomar,
 364 was not pursued in the present work, since no Pitzer parameters are available for the silica
 365 system. It has already been mentioned that Stumpf et al. reported no effect on the uptake and
 366 the spectroscopic results when adding dissolved silica to the Cm/quartz particle systems. Only
 367 when the silica concentration was raised to concentrations as high as 10 mM a significant effect
 368 was observed with quartz single crystals. The observations by Stumpf et al. are not necessarily
 369 proof for the absence of ternary silicato surface complexes in our study. Yet, the shift in the
 370 TRLFS spectra from species 1 to 2 is very similar to that observed for other oxide systems,
 371 where no ternary surface complexes were suspected⁴⁰.
 372



373 **Figure 6.** Fractional uptake of Eu ($[\text{Eu}]_{\text{T}}=1 \cdot 10^{-7}\text{M}$), S/L 10g/L, on MINUSIL as a function of pH_c
 374 and at different NaCl concentrations. Experimental data are given by symbols. Solid lines are
 375 calculations using the sub-system parameters (Tables 1 and 2) and the SCM summarized in
 376 Table 3 involving Pitzer activity coefficients for aqueous solution speciation. Dashed lines

377 represent the calculated contribution of $2(=Si_yO)HEu^{2+}$ while dashed dotted lines stand for the
378 contribution of $2(=Si_yO)EuOH^{2+}$ according to our SCM results.

379 Overall, it is concluded that the proposed model is able to describe the surface charge and Eu-
380 uptake data up to 5M NaCl concentrations. As in the case of the titrations, Figure 7 highlights
381 that the mode of presenting the data has some repercussion on how to classify the
382 observations. On the concentration scale, a clear shift in the sorption edges to higher pH_c is
383 found with increasing ionic strength (Figure 7a). On the Pitzer-activity scale, such a trend
384 cannot be clearly observed for salt contents of 1M and above (Figure 7b).
385



386 **Figure 7.** Predicted sorption edges for Eu ($[Eu]_T=1 \cdot 10^{-7} M$), S/L 10g/L, on MINUSIL as a function
387 of a) pH_c and b) pH (Pitzer pH scale) at different NaCl concentrations. Predictions obtained with
388 Table 2 - Table 3 parameters and Pitzer activity coefficients for aqueous solution speciation.

389

390 4. Conclusions

391

392 In the present study, the amphoteric quartz surface behaviour as well as the adsorption of
393 Eu(III) onto quartz surface were reported up to high ionic strengths of 5M in NaCl. An
394 electrostatic surface complexation model has been designed to describe the acid-base, zeta-
395 potential and Eu(III) uptake data in a comprehensive, self-consistent way We obtained the
396 following results:

397

398 -The titration of the quartz sample showed the clear presence of two sites from dilute to
399 concentrated conditions.

400 -The salinity effects on quartz surface charge density can be described in different ways
401 depending on the pH scale chosen. On the concentration scale a major effect occurs at acid pH
402 conditions, while on the activity scale, the effect at low pH is absent.

403 -The presence of the two sites and their concomitant surface protonation within the model
404 developed in this work is in fair agreement with previously published models covering lower
405 ionic strength conditions for quartz showing similar behaviour.
406 -Within the model, at high ionic strength ($I > 1M$), the surface potential is strongly screened by
407 ion-pair formation and the diffuse layer potential is negligibly low, which justifies the extension of
408 the standard electrostatic model to the highly saline conditions.
409 -Eu(III) sorption edges onto quartz shift towards higher pH_c with increasing ionic strength, as
410 expected based on the Eu(III) hydrolysis behaviour. As for the charging data, the chosen pH
411 scale affects the observation or not of an ionic strength effect on Eu(III) uptake.
412 -A charge distribution SCM has been fitted to the Eu(III) adsorption data involving two bidentate
413 Eu surface species.
414 -The proposed new model is in agreement with previous studies at low ionic strength conditions
415 ¹⁷, but the derived log K values differ somewhat probably related to the CD-factors and related
416 to the presence of the hydrophobic site.
417 -Coupling a Pitzer approach for the aqueous phase to a conventional surface complexation
418 model is fairly successful in describing the experimental data even when an electrostatic model
419 is used.
420 -Trivalent lanthanide uptake will be of significant importance even in solutions of high ionic
421 strengths.
422 -The model approach applied in this work can contribute to the Safety Case for nuclear waste
423 repositories in formations potentially involving high salt content.
424

425 **Acknowledgements**

426 Authors acknowledge funding from ACTINET-I3 project – Contract Number: 232631.
427

428 **References**

- 429 (1) Bradbury, M. H.; Baeyens, B. A General Application of Surface Complexation to
430 Modeling Radionuclide Sorption in Natural Systems. *J. Colloid Interface Sci.* **1993**, *158*
431 (2), 364–371.
- 432 (2) Lützenkirchen, J. Summary of Studies on (Ad) Sorption as a “Well-Established” Process
433 within FUNMIG Activities. *Appl. Geochem.* **2012**, *27* (2), 427–443.
- 434 (3) Davis, J. A.; Kent, D. B. Mineral-Water Interface Geochemistry; Hochella, F. F., White, A.
435 F., Eds.; Mineralogical Society of America, 1990; pp 177–260.
- 436 (4) Dzombak, D. A.; Morel, F. M. M. *Surface Complexation Modelling: Hydrous Ferric Oxide*;
437 Sons, J. W. &, Ed.; Wiley-Interscience, 1990.
- 438 (5) Karamalidis, A. K.; Dzombak, D. A. *Surface Complexation Modelling: Gibbsite*; John Wiley
439 & Sons, 2011.
- 440 (6) Lützenkirchen, J. *Surface Complexation Modelling*; Academic Press, 2006; Vol. 11.
- 441 (7) Mahoney J.J.; Langmuir D. Adsorption of Sr on Kaolinite, Illite and Montmorillonite at
442 High Ionic Strengths. *Radiochim. Acta* **1991**, *54* (3), 139.
443 <https://doi.org/10.1524/ract.1991.54.3.139>.
- 444 (8) Rafferty, P.; Shiao, S.-Y.; Binz, C. M.; Meyer, R. E. Adsorption of Sr(II) on Clay Minerals:
445 Effects of Salt Concentration, Loading, and PH. *J. Inorg. Nucl. Chem.* **1981**, *43* (4), 797–
446 805. [https://doi.org/https://doi.org/10.1016/0022-1902\(81\)80224-2](https://doi.org/https://doi.org/10.1016/0022-1902(81)80224-2).

- 447 (9) Hiemstra, T.; De Wit, J. C. .; Van Riemsdijk, W. . Multisite Proton Adsorption Modelling
448 at the Solid/Solution Interface of (Hydr)Oxides: A New Approach: II. Application to
449 Various Important (Hydr)Oxides. *J. Colloid Interface Sci.* **1989**, *133* (1), 105–117.
450 [https://doi.org/http://dx.doi.org/10.1016/0021-9797\(89\)90285-3](https://doi.org/http://dx.doi.org/10.1016/0021-9797(89)90285-3).
- 451 (10) Reed, D. T.; Clark, S. B.; Rao, L. *Actinide Speciation in High Ionic Strength Media:
452 Experimental and Modelling Approaches to Predicting Actinide Speciation and Migration
453 in the Subsurface*; Springer Science & Business Media, 1999.
- 454 (11) Altmaier, M.; Metz, V.; Neck, V.; Müller, R.; Fanghänel, T. Solid-liquid equilibria of
455 $Mg(OH)_2(cr)$ and $Mg_2(OH)_3Cl \cdot 4H_2O(cr)$ in the system Mg-Na-H-OH-Cl- H_2O at 25°C
456 <https://www.sciencedirect.com/science/article/pii/S0016703703001650> (accessed Mar
457 5, 2019).
- 458 (12) Domènech, C.; García, D.; Pekala, M. Decreasing K_d uncertainties through the
459 application of thermodynamic sorption models
460 <https://www.sciencedirect.com/science/article/pii/S0048969715300292> (accessed Mar
461 5, 2019).
- 462 (13) Kar, A. S.; Tomar, B. S. Cm(III) Sorption by Silica: Effect of Alpha Hydroxy Isobutyric Acid.
463 *Radiochim. Acta* **2014**, *102* (9), 763–773.
- 464 (14) Alliot, C.; Bion, L.; Mercier, F.; Toulhoat, P. Effect of Aqueous Acetic, Oxalic, and
465 Carbonic Acids on the Adsorption of Europium (III) onto α -Alumina. *J. Colloid Interface
466 Sci.* **2006**, *298* (2), 573–581.
- 467 (15) Kar, A. S.; Tomar, B. S.; Godbole, S. V.; Manchanda, V. K. Time Resolved Fluorescence
468 Spectroscopy and Modelling of Eu(III) Sorption by Silica in Presence and Absence of
469 Alpha Hydroxy Isobutyric Acid. *Colloids Surf. Physicochem. Eng. Asp.* **2011**, *378*, 44–49.
470 <https://doi.org/http://dx.doi.org/10.1016/j.colsurfa.2011.01.039>.
- 471 (16) Schnurr, A.; Marsac, R.; Rabung, T.; Lützenkirchen, J.; Geckeis, H. Sorption of Cm (III)
472 and Eu (III) onto Clay Minerals under Saline Conditions: Batch Adsorption, Laser-
473 Fluorescence Spectroscopy and Modelling. *Geochim. Cosmochim. Acta* **2015**, *151*, 192–
474 202.
- 475 (17) Stumpf, S.; Stumpf, T.; Lützenkirchen, J.; Walther, C.; Fanghänel, T. Immobilization of
476 Trivalent Actinides by Sorption onto Quartz and Incorporation into Siliceous Bulk:
477 Investigations by TRLFS. *J. Colloid Interface Sci.* **2008**, *318* (1), 5–14.
478 <https://doi.org/http://dx.doi.org/10.1016/j.jcis.2007.09.080>.
- 479 (18) Takahashi, Y.; Murata, M.; Kimura, T. Interaction of Eu(III) Ion and Non-Porous Silica:
480 Irreversible Sorption of Eu(III) on Silica and Hydrolysis of Silica Promoted by Eu(III). *J.
481 Alloys Compd.* **2006**, *408–412* (0), 1246–1251.
482 <https://doi.org/http://dx.doi.org/10.1016/j.jallcom.2005.04.120>.
- 483 (19) Schindler, P. W.; Gamsjager, H. Acid - Base Reactions of the TiO_2 (Anatase) - Water
484 Interface and the Point of Zero Charge of TiO_2 Suspensions. *Kolloid-Z. Z. Polym.* **1972**,
485 *250* (7), 759–763. <https://doi.org/10.1007/BF01498568>.
- 486 (20) Lützenkirchen, J. The Constant Capacitance Model and Variable Ionic Strength: An
487 Evaluation of Possible Applications and Applicability. *J. Colloid Interface Sci.* **1999**, *217*
488 (1), 8–18. <https://doi.org/http://dx.doi.org/10.1006/jcis.1999.6348>.
- 489 (21) Bolt, G. H. Determination of the Charge Density of Silica Sols. *J. Phys. Chem.* **1957**, *61*
490 (9), 1166–1169. <https://doi.org/10.1021/j150555a007>.
- 491 (22) Zoll, A. M.; Schifj, J. A surface complexation model of YREE sorption on *Ulva lactuca* in
492 0.05–5.0 M NaCl solutions
493 <https://www.sciencedirect.com/science/article/pii/S0016703712004802?via%3Dihub>
494 (accessed Mar 5, 2019).
- 495 (23) Guillaumont, R.; Fanghänel, T.; Fuger, J.; Grenthe, I.; Neck, V.; Palmer, D. A.; Rand, M. H.
496 *Chemical Thermodynamics 5: Update on the Chemical Thermodynamics of Uranium,
497 Neptunium, Plutonium, Americium and Technetium*; V, N. N. H. E. S. P. B., Ed.; 2003.

- 498 (24) Sverjensky, D. A.; Sahai, N. Theoretical Prediction of Single-Site Surface-Protonation
499 Equilibrium Constants for Oxides and Silicates in Water. *Geochim. Cosmochim. Acta*
500 **1996**, *60* (20), 3773–3797. [https://doi.org/http://dx.doi.org/10.1016/0016-](https://doi.org/http://dx.doi.org/10.1016/0016-7037(96)00207-4)
501 [7037\(96\)00207-4](https://doi.org/http://dx.doi.org/10.1016/0016-7037(96)00207-4).
- 502 (25) Kulik, D. Thermodynamics and Kinetics of Water-Rock Interactions; Oelkers, E. H.,
503 Schott, J., Eds.; Mineralogical Society of America, 2009; pp 125–180.
- 504 (26) Lützenkirchen, J.; Preočanin, T.; Kovačević, D.; Tomišić, V.; Lövgren, L.; Kallay, N.
505 Potentiometric Titrations as a Tool for Surface Charge Determination. *Croat. Chem. Acta*
506 **2012**, *85* (4), 391–417.
- 507 (27) Poeter, E. P.; Hill, M. C. *Documentation of UCODE: A Computer Code for Universal*
508 *Inverse Modelling*, DIANE Publishing.; 1998.
- 509 (28) Westall, J. C. *FITEQL: A Computer Program for Determination of Chemical Equilibrium*
510 *Constants from Experimental Data*; Department of Chemistry, Oregon State University,
511 1982.
- 512 (29) Ong, S.; Zhao, X.; Eisenhal, K. B. Polarization of Water Molecules at a Charged
513 Interface: Second Harmonic Studies of the Silica/Water Interface. *Chem. Phys. Lett.*
514 **1992**, *191*, 327–335. [https://doi.org/http://dx.doi.org/10.1016/0009-2614\(92\)85309-X](https://doi.org/http://dx.doi.org/10.1016/0009-2614(92)85309-X).
- 515 (30) Lützenkirchen, J. On Derivatives of Surface Charge Curves of Minerals. *J. Colloid*
516 *Interface Sci.* **2005**, *290* (2), 489–497.
517 <https://doi.org/http://dx.doi.org/10.1016/j.jcis.2005.04.074>.
- 518 (31) Allen, L. H.; Matijević, E.; Meites, L. Exchange of Na⁺ for the Silanolic Protons of Silica. *J.*
519 *Inorg. Nucl. Chem.* **1971**, *33* (5), 1293–1299.
- 520 (32) Branda, M. M.; Montani, R. A.; Castellani, N. J. The Distribution of Silanols on the
521 Amorphous Silica Surface: A Monte Carlo Simulation. *Surf. Sci.* **2000**, *446* (1–2), L89–
522 L94. [https://doi.org/http://dx.doi.org/10.1016/S0039-6028\(99\)01133-4](https://doi.org/http://dx.doi.org/10.1016/S0039-6028(99)01133-4).
- 523 (33) Krasnansky, R.; Thomas, J. K. Aminopyrene as a Monitor of Vicinal and Geminal OH
524 Groups on Silica. *Langmuir* **1994**, *10* (12), 4551–4553.
- 525 (34) Murray, D. K. Differentiating and Characterizing Geminal Silanols in Silicas by ²⁹Si NMR
526 Spectroscopy. *J. Colloid Interface Sci.* **2010**, *352* (1), 163–170.
527 <https://doi.org/http://dx.doi.org/10.1016/j.jcis.2010.08.045>.
- 528 (35) Pfeiffer-Laplaud, M.; Costa, D.; Tielens, F.; Gaigeot, M.-P.; Sulpizi, M. The Bi-Modal
529 Acidity at the Amorphous Silica/Water Interface. *J. Phys. Chem. C* **2015**.
- 530 (36) Azam, M. S.; Darlington, A.; Gibbs-Davis, J. M. The Influence of Concentration on
531 Specific Ion Effects at the Silica/Water Interface. *J. Phys. Condens. Matter* **2014**, *26* (24),
532 244107.
- 533 (37) Morag, J.; Dishon, M.; Sivan, U. The Governing Role of Surface Hydration in Ion Specific
534 Adsorption to Silica: An AFM-Based Account of the Hofmeister Universality and Its
535 Reversal. *Langmuir* **2013**, *29* (21), 6317–6322. <https://doi.org/10.1021/la400507n>.
- 536 (38) Lützenkirchen, J. Specific Ion Effects at Two Single-Crystal Planes of Sapphire. *Langmuir*
537 **2013**, *29* (25), 7726–7734. <https://doi.org/10.1021/la401509y>.
- 538 (39) James, R. O.; Healy, T. W. Adsorption of Hydrolyzable Metal Ions at the Oxide-Water
539 Interface. I. Co(II) Adsorption on SiO₂ and TiO₂ as Model Systems. *J. Colloid Interface Sci.*
540 **1972**, *40* (1), 42–52. [https://doi.org/http://dx.doi.org/10.1016/0021-9797\(72\)90172-5](https://doi.org/http://dx.doi.org/10.1016/0021-9797(72)90172-5).
- 541 (40) Geckeis, H.; Lützenkirchen, J.; Polly, R.; Rabung, T.; Schmidt, M. Mineral-Water Interface
542 Reactions of Actinides. *Chem. Rev.* **2013**, *113* (2), 1016–1062.
543 <https://doi.org/10.1021/cr300370h>.
- 544